ORGANOMETALLICS

pubs.acs.org/Organometallics Article

Ru(II)- and Os(II)-Induced Cycloisomerization of Phenol-Tethered Alkyne for Functional Chromene and Chromone Complexes

Sze-Wing Ng, Sheung-Ying Tse, Chi-Fung Yeung, Lai-Hon Chung, Man-Kit Tse, Shek-Man Yiu, and Chun-Yuen Wong*

Cite This: https://dx.doi.org/10.1021/acs.organomet.0c00048 Read Online

ABSTRACT: Diphosphine-containing Ru(II)/Os(II)−chromene and −chromone complexes were synthesized from reactions between phenol ynone HC≡C(C=O)(*o*-C_6H_4OH) and *cis*-[Ru/Os-(dppm)$_2$Cl$_2$] (dppm = 1,1-bis(diphenylphosphino)methane). The structures of these complexes in the solid state along with their pH-dependent chromene/chromone equilibrium behavior in aqueous medium were investigated. The *cis*−*trans* equilibration in solution demonstrated by chloride-ligated Ru−chromene and −chromone series represents a rare example for Ru complexes bearing dppm auxiliary ligands. More importantly, these metalated chromene and chromone complexes exhibit moderate to strong cytotoxicity against several human cancer cell lines and stronger antioxidative activities in comparison with their organic counterpart. Overall, these findings highlight the potential applications of metalated chromenes and chromones as anticancer agents and antioxidants.

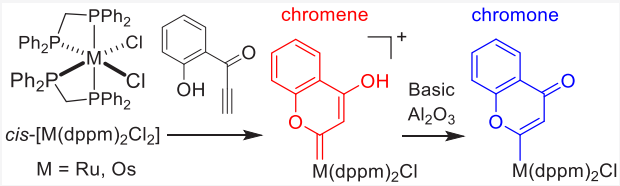

■ INTRODUCTION

Chromenes and chromones, being ubiquitous in nature, represent important pharmaceutical scaffolds for a wide range of bioactive heterocyclic compounds.[1] These heterocycles exhibit intriguing therapeutic functions, such as anticancer, antioxidative, antiviral, anti-inflammatory, and antibacterial properties.[1,2] Moreover, they have been extensively employed as light-emitting devices, fluorescence probes, and photochromic materials.[3] Therefore, there is a tremendous interest in the development of efficient synthetic methodologies to prepare new chromene and chromone derivatives.

In recent decades, various synthetic approaches utilizing functionalized alkynes as feedstocks for the preparation of organic chromenes and chromones have emerged relentlessly. For example, a variety of metal-catalyzed cyclization of alkynes have been developed for the synthesis of chromenes.[4] On the other hand, chromone derivatives can be obtained by Lewis acid/base-catalyzed cyclization of phenol-tethered alkynes.[5,6] In particular, preparation of functionalized chromones by one-pot Sonogashira carbonylation−annulation[7] has attracted considerable attention due to its mild operating conditions and convenience.

While the synthetic methodologies for organic chromenes and chromones have been well-documented for decades, the development of their transition-metalated analogues remains rare.[8] Although metalating organic heterocycles by transition metal centers represents an interesting approach to obtain novel derivatives with physical and chemical properties strikingly distinct from their corresponding organic counterparts, this research direction is dominated by transition metal−N-heterocyclic carbene (NHC) complexes,[9] whereas investigation on other metalated heterocycles is comparatively less explored due to the scarceness of general synthetic approaches.

Recently, we initiated a paradigm in preparing an array of transition-metalated heterocyclic complexes from heteroatom-functionalized alkynes and low-valent transition metal precursors. Gratifyingly, with this "metal-induced alkyne cyclization" strategy, several series of unprecedented ruthenated and osmated heterocyclic complexes were successfully isolated.[10] Herein, we report the preparation of ruthenium(II)/osmium(II)−chromene and −chromone complexes supported by the diphosphine ancillary ligand 1,1-bis-(diphenylphosphino)methane (dppm), from the reactions between *cis*-[Ru/Os(dppm)$_2$Cl$_2$] and HC≡C(C=O)(*o*-C_6H_4OH). The structures of these complexes in the solid state together with their pH-dependent chromene/chromone equilibrium behavior in aqueous medium were investigated. Interestingly, most complexes exhibit stronger cytotoxicity against several human cancer cell lines in comparison with their corresponding metal precursors and the classic anticancer drug cisplatin. Meanwhile, the noncytotoxic metalated chromene/chromone complexes possess superior antioxidative capacity when compared with their organic counterpart. To the best of our knowledge, synthesis of metalated oxycarbenes from reaction between *cis*-[M(dppm)$_2$Cl$_2$] and alcohol-

Received: January 24, 2020

tethered alkynes is rarely reported,[11] including the exploration of their potential applications. This work represents the first example of dppm-ligated metalated oxacycles with biologically relevant studies performed, including the stability of complexes in aqueous medium over a wide pH range, cytotoxicity, and antioxidative studies.

■ RESULTS AND DISCUSSION

Synthesis and Characterization. Dppm-containing Ru(II)/Os(II)−chromene/chromone complexes were prepared from reactions between *cis*-[M(dppm)$_2$Cl$_2$] (M = Ru, Os; racemic; only one enantiomer is shown in the schemes and figures) and phenol ynone HC≡C(C=O)(*o*-C$_6$H$_4$OH) with different post-transformations (Scheme 1). For the ease of discussion, the metal-ion-containing complexes isolated in this work, no matter neutral or charged, are labeled in the form of **M−L−ene** (for chromene) or **M−L−one** (for chromone), where M and L refer to the metal center (Ru, Os) and the monodentate auxiliary ligand (Cl, CH$_3$CN), respectively. Reacting *cis*-[M(dppm)$_2$Cl$_2$] and HC≡C(C=O)(*o*-C$_6$H$_4$OH) in CH$_2$Cl$_2$ with NaOTf as a mild chloride-abstracting agent under room temperature yielded monocationic complexes **Ru−Cl−ene** and **Os−Cl−ene**. These complexes could be conveniently converted into their analogous neutral chromone complexes **Ru−Cl−one** and **Os−Cl−one** by basic alumina chromatography. Both **Ru−Cl−ene** and **Ru−Cl−one** exist as a mixture of *trans* and *cis* isomers in solution as supported by ^{31}P NMR spectroscopy. Variable-temperature NMR studies revealed the temperature-dependent *cis*−*trans* equilibrium of these complexes. For instance, upon decreasing the temperature from 300 to 240 K, the *cis*/*trans* ratio of **Ru−Cl−one** in CD$_2$Cl$_2$ increased from 7/3 to 9/1. Notably, the configuration determined by X-ray crystallography does not correspond to the major isomer determined in solution by NMR spectroscopy in some cases (see below). As indicated from ^{31}P{^{1}H} NMR spectra, the unambiguously detected sharp single peak (four sets of signals) corresponding to the complexes with *trans* (*cis*) configuration strongly support the symmetric (asymmetric) nature of the complexes and are assigned to the four phosphorus atoms in the chemically equivalent (inequivalent) diphosphine ligands of the *trans* (*cis*) isomer present in the solution (see Supporting Information). On the other hand, the stereochemistry of **Os−Cl−ene** and **Os−Cl−one** in solution is comparatively less complicated. At 240−300 K, **Os−Cl−ene** and **Os−Cl−one** exist completely in *trans* and *cis* configurations, respectively. The configuration of these complexes in solution are in line with their corresponding structures obtained from X-ray crystallography (see discussion below).

Although it is well-known that reactions between *cis*-[M(dppm)$_2$Cl$_2$] (M = Ru, Os) and alkynes yield *trans*-[ClM(vinylidene)(dppm)$_2$]$^+$ complexes as products,[12] our recent studies revealed the existence of *cis*-[ClM(vinylidene)(dppm)$_2$]$^+$ intermediates: (1) *cis*-[ClM=C=CH(C=O)R(dppm)$_2$]$^+$ intermediates were formed in the reactions between *cis*-[M(dppm)$_2$Cl$_2$] (M = Ru, Os) and HC≡C(C=O)(R) to give phosphonium ring-fused bicyclic metallafuran complexes;[10h,i] (2) *cis*-[ClOs=C=CHC(OH)(2-py)$_2$ (dppm)$_2$]$^+$ was formed from the reaction between *cis*-[Os(dppm)$_2$Cl$_2$] and HC≡CC(OH)(2-py)$_2$ to give *cis*-[ClOs(indolizine)(dppm)$_2$]$^+$ complex.[10i] In comparison with these literature examples existing in either *cis* or *trans* configuration, the scenarios of *cis*−*trans* equilibrium for **Ru−Cl−ene** and **Ru−Cl−one** are rarely observed. Density functional theory (DFT) calculations were performed to compare the stability of these isomers (Table 1). Although all of the *cis*-**M−Cl−ene** and **M−Cl−one** complexes are more stable than their *trans* analogues, the energy differences are only in the range of 3−5 kcal/mol. Apparently, the calculated energy difference cannot completely account for the isomer distribution; further evaluation on the energy barriers for ligand scumbling may be required to provide a more comprehensive explanation.

Scheme 1. Synthesis of Ru(II)/Os(II)−Chromene/Chromone Complexes (*cis*/*trans* Ratio Investigated in CD$_2$Cl$_2$)

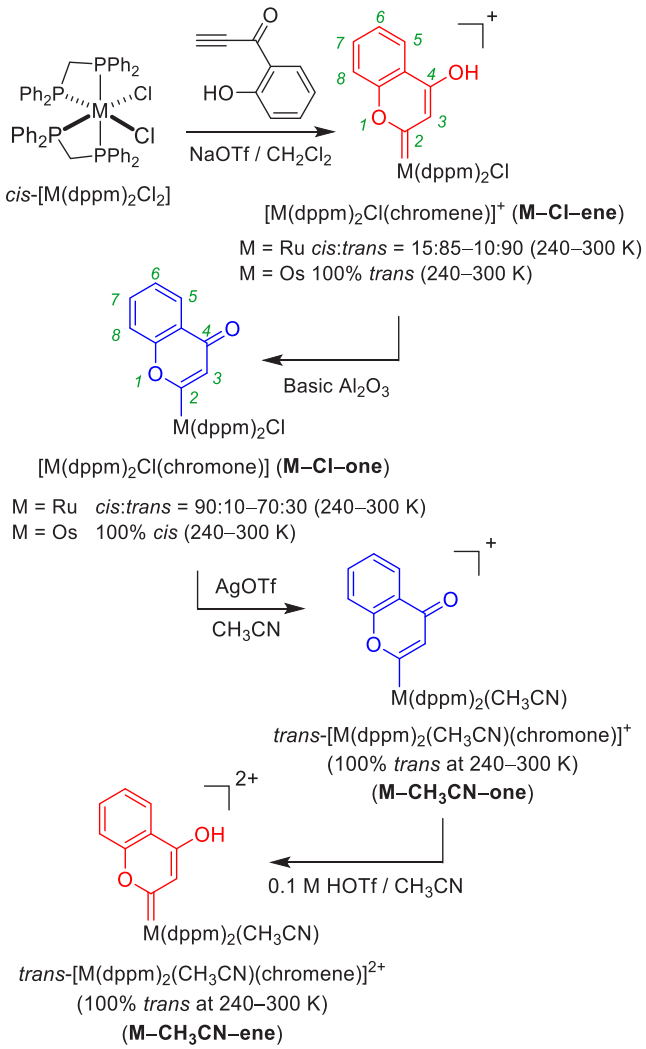

Table 1. Relative Energies of *cis*-/*trans*-M−Cl−ene and M−Cl−one Calculated at the DFT Level in Solvent (CH$_2$Cl$_2$)

complex	relative energy (kcal/mol)	
	cis configuration	*trans* configuration
Ru−Cl−ene	0.00	3.81
Ru−Cl−one	0.00	3.80
Os−Cl−ene	0.00	4.09
Os−Cl−one	0.00	5.03

https://dx.doi.org/10.1021/acs.organomet.0c00048
Organometallics XXXX, XXX, XXX−XXX

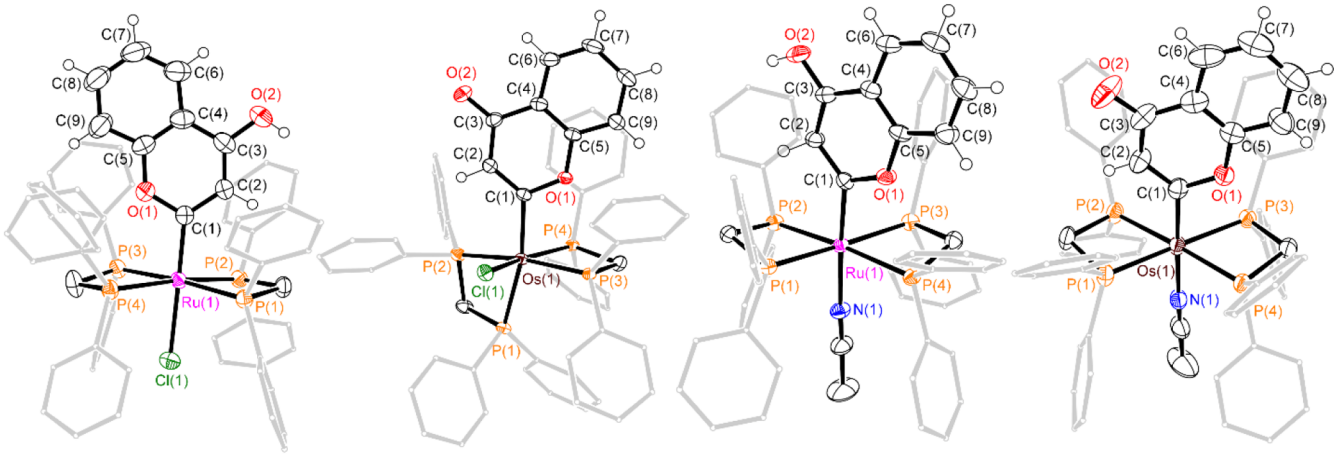

Figure 1. Perspective views of **Ru−Cl−ene**, **Os−Cl−one**, **Ru−CH$_3$CN−ene**, and **Os−CH$_3$CN−one** (from left to right) as represented by 50% probability ellipsoids (phenyl rings on dppm are represented by gray sticks for clarity).

Table 2. Selected Bond Lengths (Å) and Angles (deg) for *trans*-Ru−Cl−ene(OTf), *trans*-Os−Cl−ene(OTf), and *trans*-Ru−CH$_3$CN−ene(OTf)$_2$

complex	*trans*-**Ru−Cl−ene**(OTf)	*trans*-**Os−Cl−ene**(OTf)	*trans*-**Ru−CH$_3$CN−ene**(OTf)$_2$
M−C$_\alpha$	1.982(3)	1.9854(19)	2.014(3)
C$_\alpha$−C$_\beta$	1.414(4)	1.417(3)	1.402(4)
C$_\beta$−C$_\gamma$	1.373(5)	1.367(3)	1.379(4)
C$_\gamma$−O	1.328(4)	1.334(3)	1.325(3)
C$_\alpha$−O	1.369(4)	1.380(2)	1.369(3)
M−Cl	2.4737(7)	2.4871(5)	
M−N			2.101(2)
∠O−C$_\alpha$−C$_\beta$	115.0(3)	114.27(16)	114.6(2)
∠P(1)−M−P(2)	71.66(3)	71.016(17)	71.21(3)
∠P(3)−M−P(4)	71.49(3)	70.800(18)	70.65(3)

Table 3. Selected Bond Lengths (Å) and Angles (deg) for *trans*-Ru−Cl−one, *cis*-Os−Cl−one, *trans*-Ru−CH$_3$CN−one(OTf), and *trans*-Os−CH$_3$CN−one(OTf)

complex	*trans*-**Ru−Cl−one**[a]	*cis*-**Os−Cl−one**	*trans*-**Ru−CH$_3$CN−one**(OTf)	*trans*-**Os−CH$_3$CN−one**(OTf)
M−C$_\alpha$	2.033(3), 2.028(3)	2.0674(17)	2.046(4)	2.061(4)
C$_\alpha$−C$_\beta$	1.369(5), 1.369(4)	1.374(3)	1.366(6)	1.368(6)
C$_\beta$−C$_\gamma$	1.426(5), 1.429(5)	1.425(3)	1.408(7)	1.420(6)
C$_\gamma$−O	1.244(5), 1.239(5)	1.249(2)	1.252(6)	1.255(5)
C$_\alpha$−O	1.402(4), 1.393(4)	1.386(2)	1.386(5)	1.389(5)
M−Cl	2.4946(8), 2.4864(7)	2.4604(4)		
M−N			2.093(4)	2.084(3)
∠O−C$_\alpha$−C$_\beta$	117.0(3), 116.3(3)	116.93(15)	116.3(4)	116.6(4)
∠P(1)−M−P(2)	71.09(3), 71.45(3)	70.287(16)	71.61(4)	71.14(3)
∠P(3)−M−P(4)	71.64(3), 71.72(3)	71.883(15)	71.39(4)	70.87(3)

[a]The crystal contains two crystallographically independent metal complexes in the asymmetric unit; structural data are listed in the order of Ru(1) moiety and then Ru(2) moiety.

The CH$_3$CN-ligated chromone derivatives could be readily prepared by reacting **M−Cl−one** with chloride-abstracting agent AgOTf in CH$_3$CN at room temperature. The **M−CH$_3$CN−one** series was found to be solely in a *trans* configuration in deuterated CH$_3$CN, consistent with its structure obtained from X-ray crystallography. Direct preparation of **M−CH$_3$CN−ene** could be achieved upon acidification of **M−CH$_3$CN−one** with triflic acid during recrystallization (Scheme 1). Nevertheless, attempts to prepare **M−CH$_3$CN−ene** from **M−Cl−ene** using chloride-abstracting agent AgOTf in CH$_3$CN was unsuccessful. The ^{13}C NMR signals for the metalated carbon of chromone complexes (190−220 ppm) are consistent with those of complexes bearing a phenyl anion, whereas the metalated carbon signals of chromene complexes (226−254 ppm) are in line with those of oxycarbene complexes. All of these complexes, obtained in good to excellent yields (70−90%), are stable in ambient conditions.

The molecular structures for all isolated Ru/Os−chromene and −chromone complexes, except **Os−CH$_3$CN−ene**, were determined by X-ray crystallography (Figure 1 and Tables 2 and 3), and they represent unprecedented examples of diphosphine-containing metalated chromene and chomone complexes. Notably, the solid-state structure determined for **Os−Cl−one** was in *cis* configuration, whereas those for other

https://dx.doi.org/10.1021/acs.organomet.0c00048
Organometallics XXXX, XXX, XXX−XXX

complexes were in *trans* configurations. In particular, the *trans* configuration of **Ru−Cl−one** in the X-ray crystallographically determined molecular structure exists as a minor species in solution (*cis*/*trans* ratio = 7/3). In each case, the Ru/Os atom adopts a distorted octahedral geometry and is coordinated with a Cl/CH_3CN, two κ^2-dppm, and a monodentate chromene/chromone ligand. The metalating chromene/chromone moiety at the *C2* position of the chromene/chromone skeleton (labeled as C(1) in Figure 1) reveals its origin as a cycloisomerized HC≡C(C═O)(*o*-C_6H_4OH). Based on this premise, it is reasonable to postulate that the formation of these chromene and chromone complexes is a result of post metal−vinylidene transformation, as depicted in Scheme 2;

Scheme 2. Plausible Ru/Os−Chromene/Chromone Formation Mechanism

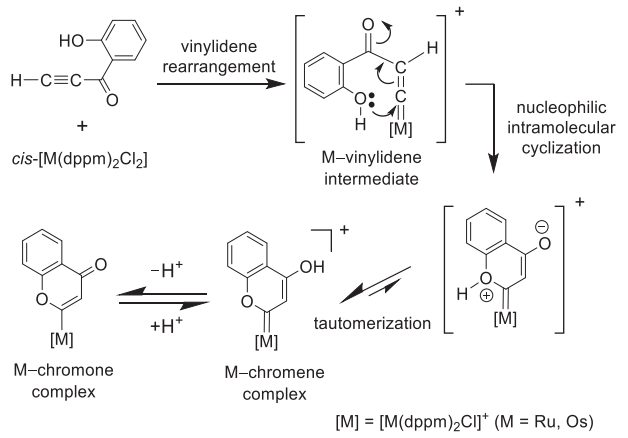

upon the formation of a metal−vinylidene intermediate from the metal precursor and the alkyne, the electrophilic C_α is attacked by the phenol moiety to form a pyran ring unit; subsequent tautomerization of this pyran ring unit yields Ru/Os−chromene complexes, and deprotonation of this metalated chromene species gives Ru/Os−chromone complexes. Although a number of recent studies reveal the existence of "non-vinylidene-involving" pathways for Ru-induced cyclization of alkynes,[13] the connectivity of the chromene/chromone moiety suggests the formation of metalated chromene and chromone complexes to be derived from vinylidene-involving pathway. It is noteworthy that the M−C distances in **Ru−Cl−one**, **Ru−CH_3CN−ene**, **Ru−CH_3CN−one**, **Os−Cl−one**, and **Os−CH_3CN−one** (2.014(3)−2.067(17) Å) are indicative of M−C single bond character, whereas those in **Ru−Cl−ene** (1.982(3) Å) and **Os−Cl−ene** (1.985(19) Å) possess partial double bond character. The angles around the C_α are consistent with sp^2 hybridization (e.g., ∠O−C_α−C_β of these complexes = 114.27(16)−117.0(3)°). The bond lengths along the C_α−C_β−C_γ−O unit of chromene and chromone complexes are consistent with an enol and enone structure, respectively. For instance, C_γ−O bond distances in **Ru−Cl−ene**, **Ru−CH_3CN−ene**, and **Os−Cl−ene** are 1.325(3)−1.334(3) Å, indicative of C−O single bond character, whereas those in **Ru−Cl−one**, **Ru−CH_3CN−one**, **Os−Cl−one**, and **Os−CH_3CN−one** are 1.239(5)−1.255(5) Å, in line with C−O double bond character.

The UV−visible spectrophotometric titrations for the determination of pK_a values were performed for all isolated Ru/Os−chromene and −chromone complexes. Well-defined isosbestic points were observed in CH_3CN-ligated Ru/Os−chromene and −chromone complexes, as depicted in Figure 2a. These findings reveal (1) quantitative conversion can be achieved between a chromene and a chromone moiety and (2) the stability of these complexes in aqueous medium over a wide pH range (pH 1−11). Meanwhile, the smaller pK_a value

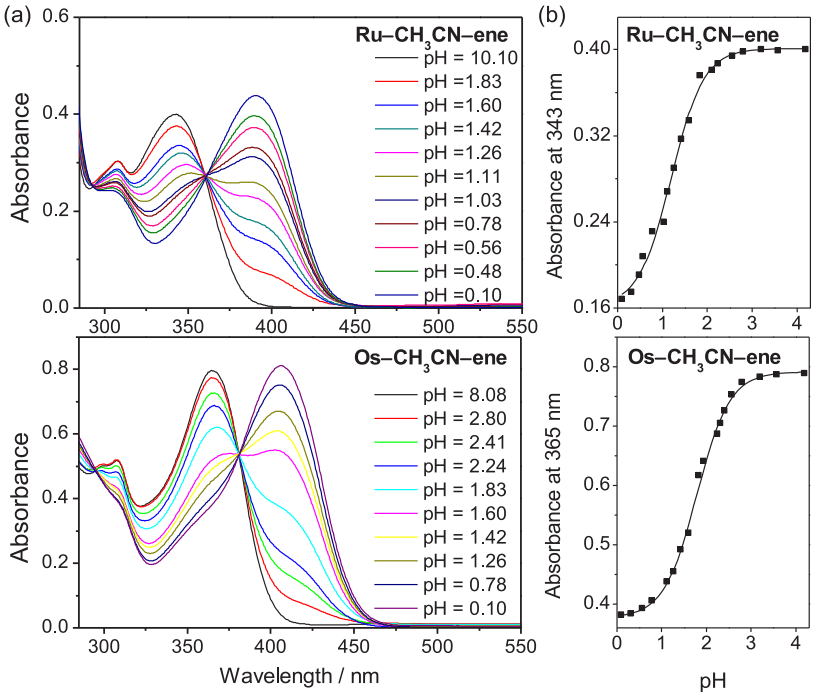

Figure 2. (a) UV−vis spectrophotometric titration spectra of **Ru−CH_3CN−ene** and **Os−CH_3CN−ene**; (b) absorbance of **Ru−CH_3CN−ene** and **Os−CH_3CN−ene** at 343 and 365 nm, respectively, as a function of pH. Counterion = OTf; spectrophotometric titrations of **Ru−CH_3CN−one** and **Os−CH_3CN−one** gave essentially the same results.

https://dx.doi.org/10.1021/acs.organomet.0c00048
Organometallics XXXX, XXX, XXX−XXX

Table 4. Cytotoxicity (IC_{50}, nM) of All Isolated Complexes, *cis*-[Ru(dppm)$_2$Cl$_2$], *cis*-[Os(dppm)$_2$Cl$_2$], and *cis*-[Pt(NH$_3$)$_2$Cl$_2$][a]

	HeLa	HT1080	MCF-7	A549
Ru−Cl−ene[b]	15200 ± 872	10600 ± 816	24300 ± 629	NC
Ru−Cl−one	11100 ± 543	10400 ± 702	46000 ± 2582	30600 ± 1570
Ru−CH$_3$CN−ene[b]	644 ± 26	261 ± 5	1095 ± 38	911 ± 35
Ru−CH$_3$CN−one[b]	500 ± 31	367 ± 18	1659 ± 199	1134 ± 34
Os−Cl−ene[b]	NC	NC	NC	NC
Os−Cl−one	NC	NC	NC	NC
Os−CH$_3$CN−ene[b]	7010 ± 129	1280 ± 37	367 ± 2	2796 ± 195
Os−CH$_3$CN−one[b]	2420 ± 297	466 ± 51	826 ± 17	2031 ± 30
cis-[Ru(dppm)$_2$Cl$_2$]	11100 ± 840	4700 ± 470	5150 ± 54	18000 ± 2110
cis-[Os(dppm)$_2$Cl$_2$]	28000 ± 3330	16900 ± 1560	24600 ± 890	68000 ± 9380
cis-[Pt(NH$_3$)$_2$Cl$_2$]	14700 ± 360	15100 ± 350	16600 ± 2460	30200 ± 4220

[a]Complex **Ru−Cl−ene** is noncytotoxic (NC) against A549 cells, and **Os−Cl−ene** and **Os−Cl−one** are NC against all cancer cell lines tested; maximum complex concentration tested: 400 μM for **Ru−Os**; 100 μM for *cis*-[Ru/Os(dppm)$_2$Cl$_2$]; 250 μM for cisplatin. [b]OTf as counterion.

of **Ru−CH$_3$CN−ene** when compared with that of **Os−CH$_3$CN−ene** (1.19 for **Ru−CH$_3$CN−ene**, 1.79 for **Os−CH$_3$CN−ene**) suggests a stronger acidic strength of the hydroxyl proton of the chromene moiety upon the change of metal center from Ru to Os (Figure 2b). On the other hand, no isosbestic points were observed in **Ru−Cl−ene** and **Ru−Cl−one**, an expected result due to the complication caused by the coexistence of *cis* and *trans* isomers and partial Cl substitution by CH$_3$CN.

Cytotoxicity Studies. The captivating anticancer properties of organic chromenes/chromones inspired us to explore the possible application of the metalated chromene/chromone complexes as anticancer agents. The in vitro anticancer activity of these complexes against cervical carcinoma (HeLa), fibrosarcoma (HT1080), breast adenocarcinoma (MCF-7), and lung adenocarcinoma (A549) human cell lines were evaluated by MTT (3-(4,5-dimethylthiazol-2-yl)-2,5-diphenyltetrazolium bromide) assay and benchmarked against the classic anticancer agent cisplatin (Table 4). In general, most complexes isolated in this work possess moderate to strong cytotoxicity against these human cancer cell lines with IC_{50} values of 0.2−46 μM. Notably, the **M−CH$_3$CN−ene** and **M−CH$_3$CN−one** showed stronger cytotoxicity in comparison with their corresponding precursors, Cl-ligated series and cisplatin, by 1−2 orders of magnitude. On the other hand, the **M−Cl−ene** and **M−Cl−one** were found to be either moderately cytotoxic or noncytotoxic. The moderate to strong cytotoxicity possessed by most of the complexes reveal their potential to be developed into practical anticancer agents.

Antioxidative Activity. Owing to the equilibration of metalated chromene and chromone complexes in aqueous medium as reflected from the spectrophotometric titration, the evaluation of antioxidative capacity was only performed for **M−Cl−one**, **M−CH$_3$CN−one**, and their organic analogue, 1,4-benzopyrone, by the DPPH (2,2-diphenyl-1-picrylhydrazyl) assay. Gratifyingly, **Ru−CH$_3$CN−one** exhibits the strongest antioxidative capacity, with the ability to scavenge 50% of the DPPH free radical (IC_{50}) at 928 ± 11 μM (Figure 3). On the other hand, the DPPH free radical scavenging activities for 1,4-benzopyrone, **M−Cl−one**, and **Os−CH$_3$CN−one** were investigated over 2 h due to their slow reaction kinetics (see Figure S3). The radical scavenging activities of the tested complexes were found to decrease in the following order: **Ru−CH$_3$CN−one** > **Ru−Cl−one** > **Os−Cl−one** > **Os−CH$_3$CN−one** > 1,4-benzopyrone. Overall, these findings indicate that metalated chromone complexes demonstrate superior antioxidative activity compared with those of their organic counterpart (1,4-benzopyrone), which exhibits negligible antioxidative capacity.

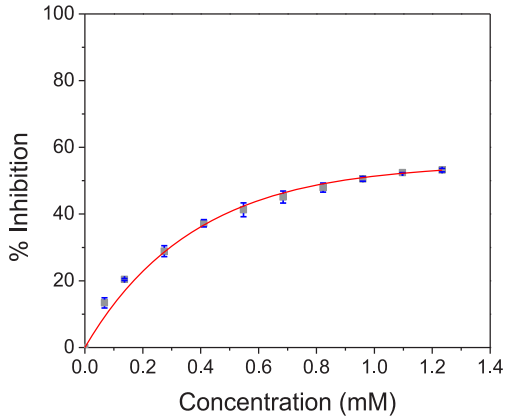

Figure 3. Free radical scavenging ability of **Ru−CH$_3$CN−one** (OTf as counterion) using the decolorization reaction of DPPH$^{\bullet}$. Data are expressed as the mean ± SD in triplicate.

■ CONCLUSION

Diphosphine-containing Ru(II)/Os(II)−chromene and −chromone complexes were prepared through activation of phenol ynone HC≡C(C=O)(*o*-C$_6$H$_4$OH) by *cis*-[Ru/Os(dppm)$_2$Cl$_2$]. The structures of these air- and moisture-stable complexes in the solid state together with their pH-dependent chromene/chromone equilibrium behavior in aqueous medium were investigated. The *cis*−*trans* equilibrium in solution exhibited by **Ru−Cl−ene** and **Ru−Cl−one** represents a rare scenario for dppm-containing Ru complexes. The moderate to strong cytotoxicity exhibited by most of the metalated chromene and chromone complexes against several human cancer cell lines highlights their potential applications as anticancer agents. Meanwhile, the finding that metalated chromone complexes possess stronger antioxidative activities in comparison to those of their organic analogue, (1,4-benzopyrone), opens new opportunities for the rational design of novel antioxidants.

■ EXPERIMENTAL SECTION

General Procedures. All reactions were performed under an argon atmosphere using standard Schlenk techniques unless otherwise stated. All reagents were used as received, and solvents for reactions were purified by a PureSolv MD5 solvent purification system. *cis*-

https://dx.doi.org/10.1021/acs.organomet.0c00048
Organometallics XXXX, XXX, XXX−XXX

Scheme 3. Labeling Scheme for H, C, and P Atoms in This Work

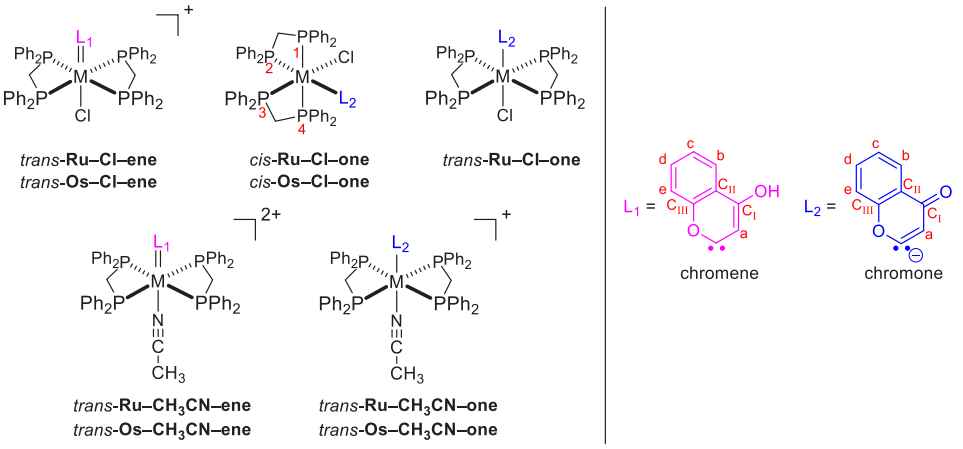

$[M(dppm)_2Cl_2]$ (racemic; M = Ru, Os; dppm = 1,1-bis-(diphenylphosphino)methane) was prepared in accordance with literature methods.[14] ^{1}H, ^{1}H{^{31}P}, ^{31}P{^{1}H}, ^{31}P, ^{13}C{^{1}H}, ^{1}H−^{1}H COSY, ^{1}H−^{1}H NOESY, ^{1}H−^{13}C HSQC, ^{1}H−^{31}P HMBC, and ^{1}H−^{13}C HMBC NMR spectra were recorded on Bruker 600 AVANCE III FT-NMR spectrometer. Peak positions were calibrated with solvent residue peaks as the internal standard. The ^{31}P{^{1}H} NMR spectra were referenced to external $P(C_6H_5)_3$ (−4.7 ppm).[15] The labeling scheme for H, C, and P atoms in the NMR assignments is shown in Scheme 3. Electrospray mass spectrometry was performed on a PE-SCIEX API 3200 triple quadrupole mass spectrometer. Elemental analyses were done on an Elementar Vario Micro Cube carbon−hydrogen−nitrogen elemental microanalyzer. UV−visible spectra were recorded on a Shimadzu UV-1800 spectrophotometer. Cell lines A549 (human lung adenocarcinoma), HT1080 (human fibrosarcoma), MCF-7 (human breast adenocarcinoma), and HeLa (human cervical carcinoma) were preserved by our laboratory. Fetal bovine serum (FBS), phosphate-buffered saline (PBS), penicillin−streptomycin (PS), trypsin-EDTA, minimum essential medium (MEM), Dulbecco's modified Eagle's medium (DMEM), and *N*-(2-hydroxyethyl)piperazine-*N*′-(2-ethanesulfonic acid) (HEPES) were purchased from Gibco BRL (Gaithersburg, MD, USA). Dimethyl sulfoxide (DMSO, >99.8%) was obtained from Acros Organics, and 3-(4,5-dimethylthiazol-2-yl)-2,5-diphenyltetrazolium bromide (MTT) was purchased from Invitrogen. 1,1-Diphenyl-2-picrylhydrazyl radical (DPPH, >97%), 2,2′-azinobis(3-ethylbenzothiazoline-6-sulfonic acid)diammonium salt (ABTS, 98%), 6-hydroxy-2,5,7,8-tetramethyl-chroman-2-carboxylic acid (Trolox, 96%), and potassium persulfate (99%) were purchased from J&K Scientific Ltd. 1,4-Benzopyrone (95%) was obtained from Fluorochem Ltd.

Synthesis of 1-(2-Hydroxyphenyl)-2-propyn-1-one. This ligand was synthesized from a modified literature procedure:[16] To a solution of salicylaldehyde (1.00 g, 8.19 mmol) in THF (20 mL) at 0 °C was added ethynylmagnesium bromide (35 mL of a 0.5 M solution in THF, 17.19 mmol) in a dropwise manner. The reaction mixture was stirred for 2 h at 0 °C and then gradually warmed to room temperature over a period of 30 min. Upon adding a saturated aqueous NH_4Cl solution (5 mL) to the reaction mixture, the aqueous layer was extracted with Et_2O (50 mL × 2) and CH_2Cl_2 (50 mL × 2). The organic phases were combined, washed with brine (50 mL × 2), dried over anhydrous $MgSO_4$, and concentrated to obtain a brown oil. 1-(2-Hydroxyphenyl)-2-propyn-1-ol was obtained after silica gel column chromatography (hexane/EtOAc: 19:1 to 17:3 (v/v)). The 1-(2-hydroxyphenyl)-2-propyn-1-ol (462 mg, 3.12 mmol) was then stirred with MnO_2 (2.17 g, 24.95 mmol) in CH_2Cl_2 at room temperature for 16 h, and the resultant brown suspension was filtered to remove brown solids. The filtrate was concentrated to give a yellow paste. 1-(2-Hydroxyphenyl)-2-propyn-1-one was obtained as yellow solids after silica gel column chromatography (hexane/CH_2Cl_2: 49:1 to 40:10 (v/v)). Yield: 1.07 g (50%).

Synthesis of M−Cl−ene(OTf). A mixture of 1-(2-hydroxyphenyl)-2-propyn-1-one (19 mg, 0.13 mmol), *cis*-$[M(dppm)_2Cl_2]$ (M = Ru/Os, 85 mg for Ru, 93 mg for Os, 0.09 mmol), and $NaCF_3SO_3$ (310 mg, 1.80 mmol) was stirred in CH_2Cl_2 (25 mL) under ambient conditions for 48 h, during which the color of the reaction mixture changed from yellow to orange. Upon filtering the mixture, the filtrate was concentrated to about 2 mL by reduced pressure and then added to Et_2O (150 mL) to give yellow precipitates. The solids (*trans*-**Ru−Cl−ene**(OTf) and *trans*-**Os−Cl−ene**(OTf)) were collected by suction filtration and washed with Et_2O (10 mL × 3). Analytically pure *trans*-**M−Cl−ene**(OTf) orange crystals were obtained by recrystallization of the precipitates (via layering of *n*-hexane onto a CH_2Cl_2 solution of the complex). Yield of **Ru−Cl−ene**(OTf): 92 mg, 85%. Anal. Calcd for $C_{60}H_{50}P_4F_3SRuClO_5$: C, 60.03; H, 4.20, N, 0.00. Found: C, 60.06; H, 4.22, N, 0.00. ^{1}H{^{31}P} NMR for *trans*-**Ru−Cl−ene**(OTf) (600 MHz, CD_2Cl_2): δ 5.08−5.15 (m, 1H, H_e), 5.28−5.39, 5.62−5.72 (m, 4H, CH_2 on P∧P), 6.81 (s, 1H, H_a), 6.86−6.93 (m, 1H, H_d), 6.97−7.05 (m, 1H, H_c), 7.59 (m, 1H, H_b), 7.11−7.17, 7.17−7.24, 7.24−7.28, 7.28−7.37, 7.47−7.65 (m, 40H, protons of Ph rings on P). ^{13}C{^{1}H} NMR for *trans*-**Ru−Cl−ene**(OTf) (150 MHz, CD_2Cl_2): δ 46.24 (CH_2 on P∧P), 115.42 (C_e), 116.54 (C_{II}), 123.58 (C_a), 123.79 (C_b), 124.97 (C_c), 131.72 (C_d), 157.05 (C_I), 160.87 (C_{III}), 254.53 (Ru−C), 128.26, 129.15, 130.12, 130.63, 132.62, 133.52, 133.69, 134.31 (48C of Ph rings on P). ^{31}P{^{1}H} NMR for *trans*-**Ru−Cl−ene**(OTf) (162 MHz, CD_2Cl_2): δ −9.07 (s, P). ^{31}P NMR (162 MHz, CD_2Cl_2): P_{cis}/P_{trans} = 1/9. The NMR spectroscopic data for *cis*-**Ru−Cl−ene**(OTf) cannot be resolved due to the trace quantities in solution. IR (KBr, cm^{-1}): ν_{O-H} = 3422. ESI-MS found (calcd): *m/z* 1051.70 (1051.45) $[C_{59}H_{50}P_4RuClO_2]^+$. Yield of **Os−Cl−ene**(OTf): 102 mg, 88%. Anal. Calcd for $C_{60}H_{50}P_4F_3SOsClO_5$: C, 55.88; H, 3.91, N, 0.00. Found: C, 55.85; H, 3.90, N, 0.00. ^{1}H{^{31}P} NMR for *trans*-**Os−Cl−ene**(OTf) (600 MHz, CD_2Cl_2): δ 5,14−5.21 (m, 1H, H_e), 5.65−5.80, 6.26−6.42 (m, 4H, CH_2 on P∧P), 6.55 (s, 1H, H_a), 6.79−6.90 (m, 1H, H_d), 6.90−6.99 (m, 1H, H_c), 7.56 (m, 1H, H_b), 10.01 (s, 1H, O*H*), 7.08−7.18, 7.18−7.23, 7.23−7.29, 7.29−7.35, 7.48−7.64 (m, 40H, protons of Ph rings on P). ^{13}C{^{1}H} NMR for *trans*-**Os−Cl−ene**(OTf) (150 MHz, CD_2Cl_2): δ 51.70 (CH_2 on P∧P), 115.06 (C_e), 116.88 (C_{II}), 123.35 (C_b), 124.54 (C_c), 125.22 (C_a), 131.15 (C_d), 157.21 (C_I), 160.62 (C_{III}), 223.81 (Os−C), 128.18, 129.03, 130.25, 130.69, 132.42, 132.64, 133.42 (48C of Ph rings on P). ^{31}P{^{1}H} NMR for *trans*-**Os−Cl−ene**(OTf) (162 MHz, CD_2Cl_2): δ −48.94 (s, P). IR (KBr, cm^{-1}): ν_{O-H} = 3446. ESI-MS found (calcd): *m/z* 1140.80 (1140.60) $[C_{59}H_{50}P_4OsClO_2]^+$.

Synthesis of M−Cl−one. A solution of **M−Cl−ene**(OTf) (48 mg for **Ru−Cl−ene**(OTf), 52 mg for **Os−Cl−ene**(OTf), 0.04 mmol) dissolved in minimal volume of CH_2Cl_2) was loaded into a CH_2Cl_2-conditioned basic alumina column. The column was eluted with a gradient of $CH_2Cl_2/(CH_3)_2CO$ mixtures (5:0 to 4:1 (v/v)). The yellow band was collected, concentrated, and added to Et_2O (150 mL) to give pale yellow precipitates. The precipitates (*trans*-**Ru−Cl−**

https://dx.doi.org/10.1021/acs.organomet.0c00048
Organometallics XXXX, XXX, XXX−XXX

one and *cis*-**Os−Cl−one**) were collected by suction filtration and washed with Et_2O (10 mL × 3). Analytically pure *trans*-**Ru−Cl−one** and *cis*-**Os−Cl−one** yellow crystals were obtained by recrystallization of the precipitates (via layering of *n*-hexane onto a CH_2Cl_2 solution of the complex). Yield of **Ru−Cl−one**: 29 mg, 70%. Anal. Calcd for $C_{59}H_{49}P_4RuClO_2$: C, 67.46; H, 4.70; N, 0.00. Found: C, 67.48; H, 4.74; N, 0.00. $^1H\{^{31}P\}$ NMR for *trans*-**Ru−Cl−one** (600 MHz, CD2Cl$_2$): δ 5.10−5.26 (m, 4H, CH_2 on P∧P), 5.26−5.38 (m, 1H, H_e), 5.56 (s, 1H, H_a), 6.71−6.81 (m, 2H, H_c & H_d), 7.51 (m, 1H, H_b), 7.12, 7.13−7.18, 7.18−7.23, 7.26−7.30, 7.37−7.40, 7.52−7.53 (m, 4oH, protons of Ph rings on P). $^1H\{^{31}P\}$ NMR for *cis*-**Ru−Cl−one** (600 MHz, CD_2Cl_2): δ 3.59−3.71, 4.14−4.27 (m, 2H, CH_2 on P_3∧P_4), 4.80−4.92, 5.10−5.26 (m, 2H, CH_2 on P_1∧P_2), 5.45−5.53 (m, 1H, H_e), 6.68−6.71 (m, 1H, H_d), 6.86−6.90 (m, 1H, H_c), 7.34 (m, 1H, H_a), 7.82 (m, 1H, H_b), 6.95, 7.02, 7.53−7.55, 7.55−7.58, 7.97, 8.32 (m, 10H, protons of Ph rings on P_1), 6.50−6.61, 6.63−6.68, 6.71−6.81, 6.99 (m, 10H, protons of Ph rings on P_2), 6.14−6.27, 6.81−6.86, 6.96, 7.01, 7.05−7.10, 7.13 (m, 10H, protons of Ph rings on P_3), 7.23−7.26, 7.34−7.36, 7.74, 8.12 (m, 10H, protons of Ph rings on P_4). $^{13}C\{^1H\}$ NMR for *trans*-**Ru−Cl−one** (150 MHz, CD_2Cl_2): δ 48.41 (CH_2 on P∧P), 115.45 (C_e), 122.12 (C_c), 123.80 (C_{II}), 124.72 (C_b), 129.46 (C_d), 131.15 (C_a), 159.46 (C_{III}), 169.29 (C_I), 217.85 (Ru−C), 127.94, 128.65, 129.55, 129.90, 132.65, 133.76, 135.63, 136,97 (48C of Ph rings on P). $^{13}C\{^1H\}$ NMR for *cis*-**Ru−Cl−one** (150 MHz, CD_2Cl_2): δ 39.64 (CH_2 on P_1∧P_2), 48.05 (CH_2 on P_3∧P_4), 115.16 (C_e), 122.56 (C_c), 124.26 (C_{II}), 124.91 (C_b), 129.18 (C_a), 129.83 (C_d), 158.84 (C_{III}), 171.45 (C_I), 220.98 (Ru−C), 128.40, 129.45, 129.72, 130.55, 131.28, 131.56, 138.32, 141.49 (12C of Ph rings on P_1), 127.49, 128.00, 128.95, 129.28, 131.41, 132.27, 136.96, 138.40 (12C of Ph rings on P_2), 127.42, 128.59, 129.05, 129.35, 130.45, 132.60, 134.21, 136.89 (12C of Ph rings on P_3), 128.46, 129.12, 130.45, 130.49, 131.80, 135.45, 136.51, 139.17 (12C of Ph rings on P_4). $^{31}P\{^1H\}$ NMR for *trans*-**Ru−Cl−one** (162 MHz, CD_2Cl_2): δ −6.74 (s, P). $^{31}P\{^1H\}$ NMR for *cis*-**Ru−Cl−one** (162 MHz, CD_2Cl_2): δ −27.49−(−26.72), −26.13−(−25.36) (m, P_1), −18.85−(−18.62) (m, P_3), −18.62−(−18.44), −17.39−(−17.12) (m, P_4), 4.63−5.45 (m, P_2). ^{31}P NMR (162 MHz, CD_2Cl_2): P_{cis}/P_{trans} = 7/3. IR (KBr, cm^{-1}): $\nu_{C=O}$ = 1603. ESI-MS found (calcd): *m/z* 1014.70 (1014.98) $[C_{59}H_{49}P_4RuO_2]^+$. Yield of **Os−Cl−one**: 36 mg, 80%. Anal. Calcd for $C_{59}H_{49}P_4OsClO_2$: C, 62.18; H, 4.33; N, 0.00. Found: C, 62.15; H, 4.32; N, 0.00. $^1H\{^{31}P\}$ NMR for *cis*-**Os−Cl−one** (600 MHz, CD_2Cl_2): δ 3.80−3.93, 5.35−5.43 (m, 2H, CH_2 on P_3∧P_4), 5.20−5.29, 5.48−5.61 (m, 2H, CH_2 on P_1∧P_2), 5.45 (m, 1H, H_e), 6.69−6.70 (m, 1H, H_d), 6.86−6.90 (m, 1H, H_c), 7.28 (m, 1H, H_a), 7.82 (m, 1H, H_b), 6.90−6.94, 6.98−7.06, 7.53, 7.59, 7.90, 8.29 (m, 10H, protons of Ph rings on P_1), 6.58, 6.64−6.69, 6.70−6.73, 6.73−6.79, 6.94−6.98 (m, 10H, protons of Ph rings on P_2), 6.26, 6.80−6.86, 6.94−6.98, 6.98−7.06, 7.06−7.20 (m, 10H, protons of Ph rings on P_3), 7.28−7.33, 7.33−7.43, 7.77, 8.11 (m, 10H, protons of Ph rings on P_4). $^{13}C\{^1H\}$ NMR for *cis*-**Os−Cl−one** (150 MHz, CD_2Cl_2): δ 47.19 (CH_2 on P_3∧P_4), 53.37 (CH_2 on P_1∧P_2), 115.21 (C_e), 122.41 (C_c), 124.15 (C_{II}), 124.68 (C_b), 129.20 (C_a), 129.69 (C_d), 158.94 (C_{III}), 173.04 (C_I), 201.32 (Os−C), 128.29, 129.35, 129.63, 130.59, 131.01, 131.16, 138.13, 142.67 (12C of Ph rings on P_1), 127.25, 127.84, 128.75, 129.12, 131.08, 131.93, 136.56, 137.85 (12C of Ph rings on P_2), 127.18, 128.75, 128.97, 129.56, 130.15, 132.59, 133.59, 135.68 (12C of Ph rings on P_3), 128.37, 129.04, 130.45, 130.52, 131.65, 135.19, 136.70, 139.32 (12C of Ph rings on P_4). $^{31}P\{^1H\}$ NMR for *cis*-**Os−Cl−one** (162 MHz, CD_2Cl_2): δ −69.13−(−68.74), −68.00−(−67.50) (m, P1), −63.84−(−63.55), −62.62−(−62.36) (m, P_4), −51.88−(−51.54) (m, P_3), −49.72−(−49.25) (m, P_2). IR (KBr, cm^{-1}): $\nu_{C=O}$ = 1607. ESI-MS found (calcd): *m/z* 1104.40 (1104.14) $[C_{59}H_{49}P_4OsO_2]^+$.

Synthesis of M−CH_3CN−ene(OTf)$_2$. Analytically pure *trans*-**M−CH_3CN−ene**(OTf)$_2$ white crystals were obtained by recrystallization of the precipitates (via slow diffusion of Et_2O into a 0.1 M HOTf-treated CH_3CN solution of **M−CH_3CN−one**(OTf) (35 mg for **Ru−CH_3CN−one**(OTf), 38 mg for **Os−CH_3CN−one**(OTf), 0.03 mmol). Yield of **Ru−CH_3CN−ene**(OTf)$_2$: 37 mg, 90%. Anal. Calcd for $C_{63}H_{53}NP_4F_6S_2RuO_8$: C, 55.84; H, 3.94; N, 1.03. Found: C, 55.81; H, 3.97; N, 1.05. $^1H\{^{31}P\}$ NMR for *trans*-**Ru−CH_3CN−ene**(OTf)$_2$ (600 MHz, CD_3CN): δ 0.92 (s, 3H, CH_3CN), 5.48−5.71 (m, 4H, CH_2 on P∧P), 6.20−6.37 (m, 1H, H_e), 7.02 (s, 1H, H_a), 7.35 (m, 1H, H_c), 7.36 (m, 1H, H_d), 7.76−7.89 (m, 1H, H_b), 7.14−7.24, 7.25−7.33, 7.33−7.42, 7.47−7.54 (m, 40H, protons of Ph rings on P). $^{13}C\{^1H\}$ NMR for *trans*-**Ru−CH_3CN−ene**(OTf)$_2$ (150 MHz, CD_3CN): δ 47.43 (CH_2 on P∧P), 117.01 (C_e), 120.98(C_{II}), 124.57 (C_a), 124.91 (C_b), 127.33 (C_c), 130.47 (CH_3CN), 135.03 (C_d), 161.59 (C_I), 162.10 (C_{III}), Ru−C (cannot be resloved), 129.92, 130.08, 132.15, 132.21, 132.24, 133.07, 133.19 (48C of Ph rings on P). $^{31}P\{^1H\}$ NMR for *trans*-**Ru−CH_3CN−ene**(OTf)$_2$ (162 MHz, CD_3CN): δ −9.93 (s, P). IR (KBr, cm^{-1}): $\nu_{C=O}$ = 3421. ESI-MS found (calcd): *m/z* 1206.70 (1206.11) $[C_{62}H_{53}NP_4F_3SRuO_5]^+$. Yield of **Os−$CH_3CN$−ene**(OTf)$_2$: 37 mg, 90%. Anal. Calcd for $C_{63}H_{53}NP_4F_6S_2OsO_8$: C, 52.39; H, 3.70; N, 0.97. Found: C, 52.36; H, 3.73; N, 0.95. $^1H\{^{31}P\}$ NMR for *trans*-**Os−CH_3CN−ene**(OTf)$_2$ (600 MHz, CD_3CN): δ 1.14 (s, 3H, protons of CH_3CN), 5.92−6.06, 6.35−6.46 (m, 4H, CH_2 on P∧P), 6.53−6.61 (m, 1H, H_b), 6.91 (s, 1H, H_a), 7.28−7.32 (m, 1H, H_d), 7.34−7.37 (m, 1H, H_c), 7.74−7.83 (m, 1H, H_e), 7.15−7.27, 7.34−7.42, 7.46−7.59 (m, 40H, protons of Ph rings on P). $^{13}C\{^1H\}$ NMR for *trans*-**Os−CH_3CN−ene**(OTf)$_2$ (150 MHz, CD_3CN): δ 3.68 (CH_3CN), 53.26 (CH_2 on P∧P), 116.65 (C_{II}), 116.81 (C_b), 124.50 (C_e), 125.78 (C_a), 127.18 (C_d), 127.71 (CH_3CN), 134.80 (C_c), 161.30 (C_I), 161.71 (C_{III}), 226.61 (Os−C), 129.82, 130.09, 130.86, 131.15, 131.31, 132.40, 132.80, 133.13 (48C of Ph rings on P). $^{31}P\{^1H\}$ NMR for *trans*-**Os−CH_3CN−ene**(OTf)$_2$ (162 MHz, CD_3CN): δ −49.45 (s, P). IR (KBr, cm^{-1}): $\nu_{C=O}$ = 3422. ESI-MS found (calcd): *m/z* 1295.70 (1295.27) $[C_{62}H_{53}NP_4F_3SOsO_5]^+$.

Synthesis of M−CH_3CN−one(OTf). To a 25 mL CH_3CN solution of **M−Cl−one** (80 mg for **Ru−Cl−one**, 91 mg for **Os−Cl−one**, 0.08 mmol) was added AgOTf (23 mg, 0.09 mmol), and this mixture was stirred at room temperature under argon for 16 h, during which the color of the reaction mixture changed from yellow to pale yellow. Upon centrifugation for removal of AgCl, the supernatant was collected and concentrated to about 2 mL by reduced pressure and then added to Et_2O (150 mL) to give pale yellow precipitates. The solids (*trans*-**Ru−CH_3CN−one**(OTf) and *trans*-**Os−CH_3CN−one**(OTf)) were collected by suction filtration and washed with Et_2O (10 mL × 3). Analytically pure *trans*-**M−CH_3CN−one**(OTf) white crystals were obtained by recrystallization of the precipitates (via slow diffusion of Et_2O into a CH_3CN solution of the complex). Yield of **Ru−CH_3CN−one**(OTf): 84 mg, 87%. Anal. Calcd for $C_{62}H_{52}NP_4F_3SRuO_5$: C, 61.79; H, 4.35; N, 1.16. Found: C, 61.78; H, 4.32; N, 1.13. $^1H\{^{31}P\}$ NMR for *trans*-**Ru−CH_3CN−one**(OTf) (600 MHz, CD_3CN): δ 5.20−5.29, 5.36−5.46 (m, 4H, CH_2 on P∧P), 5.31 (m, 1H, H_e), 6.04 (s, 1H, H_a), 7.00 (m, 1H, H_d), 7.06 (m, 1H, H_c), 7.73 (m, 1H, H_b), 7.10−7.19, 7.26−7.42, 7.42−7.54 (m, 40H, protons of Ph rings on P). $^{13}C\{^1H\}$ NMR for *trans*-**Ru−CH_3CN−one**(OTf) (150 MHz, CD_3CN): δ 47.86 (CH_2 on P∧P), 116.71 (C_e), 124.05 (C_c), 124.29 (C_{II}), 125.44 (C_b), 130.74 (C_a), 131.72 (C_d), 160.29 (C_{III}), 171.59 (C_I), 211.68 (Ru−C), 129.41, 129.69, 131.51, 131.63, 133.10, 133.21, 133.40, 134.00 (48C of Ph rings on P). $^{31}P\{^1H\}$ NMR for *trans*-**Ru−CH_3CN−one**(OTf) (162 MHz, CD_3CN): δ − 6.64 (s, P). IR (KBr, cm^{-1}): $\nu_{C=O}$ = 1607. ESI-MS found (calcd): *m/z* 1014.70 (1014.98) $[C_{59}H_{49}P_4RuO_2]^+$. Yield of **Os−CH_3CN−one**(OTf): 91 mg, 88%. Anal. Calcd for $C_{62}H_{52}NP_4F_3SOsO_5$: C, 57.54; H, 4.05; N, 1.08. Found: C, 57.51; H, 4.08; N, 1.06. $^1H\{^{31}P\}$ NMR for *trans*-**Os−CH_3CN−one**(OTf) (600 MHz, CD_3CN): δ 0.88 (s, 3H, CH_3CN), 5.49−5.59, 6.27−6.39 (m, 4H, CH_2 on P∧P), 5.59−5.66 (m, 1H, H_e), 6.12 (s, 1H, H_a), 6.94−7.07 (m, 2H, H_c & H_d), 7.68−7.74 (m, 1H, H_b), 7.07−7.19, 7.24−7.29, 7.29−7.33, 7.33−7.38, 7.41−7.52 (m, 40H, protons of Ph rings on P). $^{13}C\{^1H\}$ NMR for *trans*-**Os−CH_3CN−one**(OTf) (150 MHz, CD_3CN): δ 2.95 (CH_3CN), 53.95 (CH_2 on P∧P), 116.49 (Ce), 122.55 (CH_3CN), 123.91 (C_c), 124.24 (C_{II}), 125.30 (C_b), 130.85 (C_a), 131.63 (C_d), 160.17 (C_{III}), 172.73 (C_I), 190.41 (Os−C), 129.30, 129.65, 131.63, 131.75, 132.00, 132.95, 133.14, 133.19 (48C of Ph rings on P). $^{31}P\{^1H\}$ NMR for *trans*-**Os−CH_3CN−one**(OTf) (162 MHz,

https://dx.doi.org/10.1021/acs.organomet.0c00048
Organometallics XXXX, XXX, XXX−XXX

CD_3CN): δ − 48.07 (s, P). IR (KBr, cm^{-1}): $\nu_{C=O}$ = 1606. ESI-MS found (calcd): m/z 1104.70 (1104.14) $[C_{59}H_{49}P_4RuO_2]^+$.

Variable-Temperature NMR Spectroscopy. The variable-temperature NMR spectra were acquired using a Bruker 600 AVANCE III FT-NMR spectrometer. Probe temperatures (±0.5 K) were measured with a calibrated digital thermocouple. Samples were allowed to equilibrate for 10 min at each temperature before recording the $^{31}P\{^1H\}$ spectrum of metalated chromene/chromone complexes.

Detemination of pK_a Values. UV−visible absorption measurements were performed on **M−CH_3CN−one**(OTf) in various pH aqueous solutions to determine their pK_a values. Each spectrum, recorded at 298 K, was obtained from a mixture of aqueous solution (1.60 mL for **Ru−CH_3CN−one**(OTf), 2.10 mL for **Os−CH_3CN−one**(OTf)) with fixed pH values (ranging from 1 to 11, prepared by adding HCl or NaOH to deionized water) and CH_3CN solution of **Ru−CH_3CN−one**(OTf) (1.00 mL, 0.08 mM) or **Os−CH_3CN−one**(OTf) (0.5 mL, 0.27 mM). The pK_a values were determined from the inflection points in Figure 2b.

Cytotoxicity Activity in Vitro by MTT Assay. The cytotoxicity of all complexes (OTf as counterion for charged complexes), *cis*-$[Ru(dppm)_2Cl_2]$, *cis*-$[Os(dppm)_2Cl_2]$, and *cis*-$[Pt(NH_3)_2Cl_2]$ against A549, HT1080, MCF-7, and HeLa cancer cells was evaluated using the MTT assay.[17] Briefly, cells (A549, HT1080, MCF-7 and HeLa) were seeded at a specific amount (14000 cells per well for A549; 5000 cells per well for HT1080; 10000 cells per well for MCF-7; 5000 cells per well for HeLa) in a 96-well culture microplate using 100 μL of 10% FBS and 1% PS MEM supplemented with 10 mM HEPES for A549 cells or 100 μL of 10% FBS and 1% PS DMEM for HT1080, MCF-7, and HeLa cells as culture solution and incubated for 24 h at standard incubation conditions for mammalian cells (37 °C, 5% CO_2, 95% air). Stock solutions of all complexes (10 mM), *cis*-$[Ru(dppm)_2Cl_2]$ and *cis*-$[Os(dppm)_2Cl_2]$ (5 mM), were prepared using DMSO as solvent, whereas that of cisplatin (1 mM) was prepared using 0.9% (w/v) saline solution as the solvent. A series of concentrations for all complexes (1.53 nM to 400 μM), *cis*-$[M(dppm)_2Cl_2]$ (M = Ru and Os) (0.19 nM to 100 μM) and *cis*-$[Pt(NH_3)_2Cl_2]$ (0.48 nM to 250 μM), were prepared in 100 μL of 1% FBS and 1% PS MEM supplemented with HEPES or DMEM and added to each well. For all synthesized complexes, the highest concentration of complex-treated cell culture medium constitutes 4% DMSO. For *cis*-$[Ru(dppm)_2Cl_2]$ and *cis*-$[Os(dppm)_2Cl_2]$, the highest concentration of complex-treated cell culture medium constitutes 1% DMSO. For the corresponding control experiments, 4 and 1% DMSO were used, respectively. The microplate was incubated for 48 h. Afterward, the complex-containing culture medium was replaced by MTT reagent (5 mg/mL in PBS), and the microplate was incubated for 4 h. Upon incubation, the PBS medium was removed and 100 μL of DMSO was added to dissolve the formazan for absorbance measurement at 570 nm using a microplate reader. The cytotoxicity of each complex, expressed as IC_{50}, was determined by the surviving cells curve after exposure to complexes for 48 h. Each experiment was repeated three times to obtain the mean values.

Free Radical Scavenging Activity by DPPH Assay.[18] The stock solutions of different samples were freshly prepared in MeOH (0.79 mM for DPPH, 1.49 mM for **Ru−CH_3CN−one**(OTf), 0.35 mM for 1,4-benzopyrone, **Ru−Cl−one**, **Os−Cl−one**, and **Os−CH_3CN−one**(OTf)) and incubated for at least 30 min prior to any measurement. The free radical scavenging activity for **Ru−CH_3CN−one**(OTf) was determined by adding various amounts of stock MeOH solutions of **Ru−CH_3CN−one**(OTf) to 100 μL of the working DPPH solution and made up to 1100 μL with MeOH so that the final concentration of the samples ranged from 0 to 1.23 mM. The DPPH free radical scavenging activities for remaining samples were investigated for 2 h due to the slow reaction kinetics. The free radical scavenging activity for a sample at time t was determined using the equation $[A_{control}(t) - A_{sample}(t)]/A_{control}(t) \times 100\%$ (where $A_{control}(t)$ is the absorbance at 517 nm at time t for a mixture of 100 μL of MeOH solution of DPPH and 1000 μL of MeOH; $A_{sample}(t)$ is the absorbance at 517 nm at time t for a mixture of 100 μL of MeOH solution of DPPH with various amount of **Ru−CH_3CN−one**(OTf) (or 808 μL of stock MeOH solution of remaining samples) and MeOH). The antioxidative capacity of **Ru−CH_3CN−one**(OTf) and remaining samples is shown in Figures 3 and S3, respectively.

■ ASSOCIATED CONTENT

Supporting Information

The Supporting Information is available free of charge at https://pubs.acs.org/doi/10.1021/acs.organomet.0c00048.

NMR spectra for all the complexes reported in this work, computational methodology, additional X-ray figures, and antioxidative studies (PDF)

Cartesian coordinates of calculated structures in this work (XYZ)

Accession Codes

CCDC 1979800−1979806 contain the supplementary crystallographic data for this paper. These data can be obtained free of charge via www.ccdc.cam.ac.uk/data_request/cif, or by emailing data_request@ccdc.cam.ac.uk, or by contacting The Cambridge Crystallographic Data Centre, 12 Union Road, Cambridge CB2 1EZ, UK; fax: +44 1223 336033.

■ AUTHOR INFORMATION

Corresponding Author

Chun-Yuen Wong − *Department of Chemistry and State Key Laboratory of Terahertz and Millimeter Waves, City University of Hong Kong, Kowloon, Hong Kong SAR;* orcid.org/0000-0003-4780-480X; Email: acywong@cityu.edu.hk

Authors

Sze-Wing Ng − *Department of Chemistry and State Key Laboratory of Terahertz and Millimeter Waves, City University of Hong Kong, Kowloon, Hong Kong SAR*

Sheung-Ying Tse − *Department of Chemistry, City University of Hong Kong, Kowloon, Hong Kong SAR*

Chi-Fung Yeung − *Department of Chemistry and State Key Laboratory of Terahertz and Millimeter Waves, City University of Hong Kong, Kowloon, Hong Kong SAR*

Lai-Hon Chung − *Department of Chemistry, City University of Hong Kong, Kowloon, Hong Kong SAR*

Man-Kit Tse − *Department of Chemistry, City University of Hong Kong, Kowloon, Hong Kong SAR*

Shek-Man Yiu − *Department of Chemistry, City University of Hong Kong, Kowloon, Hong Kong SAR*

Complete contact information is available at: https://pubs.acs.org/10.1021/acs.organomet.0c00048

Notes

The authors declare no competing financial interest.

■ ACKNOWLEDGMENTS

The work described in this paper was supported by the Hong Kong Innovation and Technology Commission (ITS/265/17FP) and the Research Grants Council of Hong Kong SAR (CityU 11228316, CityU 11207117, and T42-103/16-N).

■ REFERENCES

(1) (a) Horton, D. A.; Bourne, G. T.; Smythe, M. L. The Combinatorial Synthesis of Bicyclic Privileged Structures or Privileged Substructures. *Chem. Rev.* **2003**, *103*, 893−930. (b) Gaspar, A.; Matos, M. J.; Garrido, J.; Uriarte, E.; Borges, F. Chromone: A Valid Scaffold in Medicinal Chemistry. *Chem. Rev.* **2014**, *114*, 4960−4992. (c) Keri, R. S.; Budagumpi, S.; Pai, R. K.; Balakrishna, R. G.

Chromones as a privileged scaffold in drug discovery: A review. *Eur. J. Med. Chem.* **2014**, *78*, 340−374. (d) Silva, C. F. M.; Pinto, D. C. G. A.; Silva, A. M. S. Chromones: A Promising Ring System for New Antiinflammatory Drugs. *ChemMedChem* **2016**, *11*, 2252−2260.

(2) (a) Edwards, A. M.; Howell, J. B. L. The chromones: history, chemistry and clinical development. A tribute to the work of Dr R. E. C. Altounyan. *Clin. Exp. Allergy* **2000**, *30*, 756−774. (b) Birt, D. F.; Hendrich, S.; Wang, W. Dietary agents in cancer prevention: flavonoids and isoflavonoids. *Pharmacol. Ther.* **2001**, *90*, 157−177. (c) Kim, H. P.; Son, K. H.; Chang, H. W.; Kang, S. S. Anti-inflammatory Plant Flavonoids and Cellular Action Mechanisms. *J. Pharmacol. Sci.* **2004**, *96*, 229−245. (d) Kosmider, B.; Osiecka, R. Flavonoid Compounds: A Review of Anticancer Properties and Interactions with *cis*-Diamminedichloroplatinum(II). *Drug Dev. Res.* **2004**, *63*, 200−211. (e) K. Sharma, S.; Kumar, S.; Chand, K.; Kathuria, A.; Gupta, A.; Jain, R. An Update on Natural Occurrence and Biological Activity of Chromones. *Curr. Med. Chem.* **2011**, *18*, 3825−3852. (f) Patil, S. A.; Patil, R.; Pfeffer, L. M.; Miller, D. D. Chromenes: potential new chemotherapeutic agents for cancer. *Future Med. Chem.* **2013**, *5*, 1647−1660. (g) Pratap, R.; Ram, V. J. Natural and Synthetic Chromenes, Fused Chromenes, and Versatility of Dihydrobenzo[h]chromenes in Organic Synthesis. *Chem. Rev.* **2014**, *114*, 10476−10526. (h) Costa, M.; Dias, T. A.; Brito, A.; Proença. Biological importance of structurally diversified chromenes. *Eur. J. Med. Chem.* **2016**, *123*, 487−507. (i) Varela, J. A.; Saá. Metal-Catalyzed Cyclizations to Pyran and Oxazine Derivatives. *Synthesis* **2016**, *48*, 3470−3478. (j) Santos, C. M. M.; Silva, A. M. S. An Overview of 2-Styrylchromones: Natural Occurrence, Synthesis, Reactivity and Biological Properties. *Eur. J. Org. Chem.* **2017**, *2017*, 3115−3133. (k) Sadek, K. U.; Mekheimer, R. A. H.; Abd-Elmonem, M.; Abdel-Hameed, A.; Elnagdi, M. H. Recent developments in the enantioselective synthesis of polyfunctionalized pyran and chromene derivatives. *Tetrahedron: Asymmetry* **2017**, *28*, 1462−1485.

(3) (a) Chen, F.-T. Evolution of Red Organic Light-Emitting Diodes: Materials and Devices. *Chem. Mater.* **2004**, *16*, 4389−4400. (b) Sousa, C. M.; Pina, J.; Seixas de Melo, J.; Berthet, J.; Delbaere, S.; Coelho, P. J. Synthesis of a Photochromic Fused 2*H*-Chromene Capable of Generating a Single Coloured Species. *Eur. J. Org. Chem.* **2012**, *2012*, 1768−1773. (c) Yoon, J.-Y.; Lee, J. S.; Yoon, S. S.; Kim, Y. K. Red Fluorescent Donor-π-Acceptor Type Materials based on Chromene Moiety for Organic Light-Emitting Diodes. *Bull. Korean Chem. Soc.* **2014**, *35*, 1670−1674. (d) Li, C.-R.; Li, S.-L.; Yang, Z.-Y. A chromone-derived Schiff-base as Al^{3+} "turn-on" fluorescent probe based on photoinduced electron-transfer (PET) and C═N isomerization. *Tetrahedron Lett.* **2016**, *57*, 4898−4904. (e) Yan, J.; Fan, L.; Qin, J.-c.; Li, C.-r.; Yang, Z.-y. A Novel Chromone Schiff-Base Fluorescent Chemosensor for Cd(II) Based on C═N Isomerization. *J. Fluoresc.* **2016**, *26*, 1059−1065. (f) Namba, T.; Hayashi, Y.; Kawauchi, S.; Shibata, Y.; Tanaka, K. Rhodium-Catalyzed Cascade Synthesis of Benzofuranylmethylidene-Benzoxasiloles: Elucidating Reaction Mechanism and Efficient Solid-State Fluorescence. *Chem. - Eur. J.* **2018**, *24*, 7161−7171. (g) Li, C.-R.; Li, S.-L.; Wang, G.-Q.; Yang, Z.-Y. Spectroscopic properties of a chromone-fluorescein conjugate as Mg^{2+} "turn on" fluorescent probe. *J. Photochem. Photobiol., A* **2018**, *356*, 700−707. (h) Liu, L.-M.; Yang, Z.-Y. *J. Photochem. Photobiol., A* **2018**, *364*, 558−563. (i) Xue, J.; Tian, L.-M.; Yang, Z.-Y. A novel rhodamine-chromone Schiff-base as turn-on fluorescent probe for the detection of Zn(II) and Fe(III) in different solutions. *J. Photochem. Photobiol., A* **2019**, *369*, 77−84. (j) Tian, L.-M.; Xue, J.; Li, S.-L.; Yang, Z.-Y. A novel chromone derivative as dual probe for selective sensing of Al(III) by fluorescent and Cu(II) by colorimetric methods in aqueous solution. *J. Photochem. Photobiol., A* **2019**, *382*, 111955−111962. (k) Pang, B.-J.; Li, C.-R.; Yang, Z.-Y. A novel chromone and rhodamine derivative as fluorescent probe for the detection of Zn(II) and Al(III) based on two different mechanisms. *Spectrochim. Acta, Part A* **2018**, *204*, 641−647. (l) Fan, L.; Qin, J.-C.; Li, C.-R.; Yang, Z.-Y. A Schiff-base receptor based chromone derivate: Highly selective fluorescent and colorimetric probe for Al(III). *Spectrochim. Acta, Part A* **2019**, *218*, 342−347.

(4) (a) Pastine, S. J.; Youn, S. W.; Sames, D. Pt^{IV}-Catalyzed Cyclization of Arene-Alkyne Substrates via Intramolecular Electrophilic Hydroarylation. *Org. Lett.* **2003**, *5*, 1055−1058. (b) Nevado, C.; Echavarren, A. M. Intramolecular Hydroarylation of Alkynes Catalyzed by Platinum or Gold: Mechanism and endo Selectivity. *Chem. - Eur. J.* **2005**, *11*, 3155−3164. (c) Xia, X.-F.; Song, X.-R.; Liu, X.-Y.; Liang, Y.-M. Lewis Acid-Catalyzed Intramolecular [3 + 2] Cycloaddition of Cyclopropane 1,1-Diesters with Alkynes for the Synthesis of Cyclopenta[c]chromene Skeletons. *Chem. - Asian J.* **2012**, *7*, 1538−1541. (d) Shiva Kumar, K.; Rambabu, D.; Prasad, B.; Mujahid, M.; Krishna, G. R.; Basaveswara Rao, M. V.; Malla Reddy, C.; Vanaja, G. R.; Kalle, A. M.; Pal, M. A new approach to construct a fused 2-ylidene chromene ring: highly regioselective synthesis of novel chromeno quinoxalines. *Org. Biomol. Chem.* **2012**, *10*, 4774−4781. (e) Dorel, R.; Echavarren, A. M. Gold(I)-Catalyzed Activation of Alkynes for the Construction of Molecular Complexity. *Chem. Rev.* **2015**, *115*, 9028−9072. (f) Majumdar, N.; Paul, N. D.; Mandal, S.; de Bruin, B.; Wulff, W. D. Catalytic Synthesis of 2*H*-Chromenes. *ACS Catal.* **2015**, *5*, 2329−2366. (g) Shang, X. S.; Li, N. T.; Li, D. Y.; Liu, P. N. Palladium-Catalyzed Tandem Reaction of Alkyne-Based Aryl Iodides and Salicyl *N*-Tosylhydrazones to Construct the Spiro-[benzofuran-3,2′-chromene] Skeleton. *Adv. Synth. Catal.* **2016**, *358*, 1577−1582. (h) Zhao, Y.-S.; Yu, C.-G.; Wang, T.-B.; She, Z.-J.; Zheng, X.-S.; You, J.-S.; Gao, Ge. Tandem Rh-Catalyzed [4 + 2] Vinylic C-H O-Annulation of Exocyclic Enones with Alkynes and 1,5-H Shift. *Org. Lett.* **2018**, *20*, 1074−1077. (i) Perez Sestelo, J.; Sarandeses, L. A.; Martinez, M. M.; Alonso-Maranon, L. *Org. Biomol. Chem.* **2018**, *16*, 5733−5747. (j) Panda, N.; Mattan, I.; Ojha, S.; Purohit, C. S. Synthesis of medium-sized (6−7−6) ring compounds by iron-catalyzed dehydrogenative C−H activation/annulation. *Org. Biomol. Chem.* **2018**, *16*, 7861−7870. (k) Dutta, P. K.; Ravva, M. K.; Sen, S. Cobalt-Catalyzed, Hydroxy-Assisted C−H Bond Functionalization: Access to Diversely Substituted Polycyclic Pyrans. *J. Org. Chem.* **2019**, *84*, 1176−1184.

(5) (a) Zhou, C.; Dubrovsky, A. V.; Larock, R. C. Diversity-Oriented Synthesis of 3-Iodochromones and Heteroatom Analogues via ICl-Induced Cyclization. *J. Org. Chem.* **2006**, *71*, 1626−1632. (b) Silva, F.; Reiter, M.; Mills-Webb, R.; Sawicki, M.; Klär, D.; Bensel, N.; Wagner, A.; Gouverneur, V. Pd(II)-Catalyzed Cascade Wacker-Heck Reaction: Chemoselective Coupling of Two Electron-Deficient Reactants. *J. Org. Chem.* **2006**, *71*, 8390−8394. (c) Ahmed, N.; Dubuc, C.; Rousseau, J.; Bénard, F.; van Lier, J. E. Synthesis, characterization, and estrogen receptor binding affinity of flavone-, indole-, and furan-estradiol conjugates. *Bioorg. Med. Chem. Lett.* **2007**, *17*, 3212−3216. (d) Harkat, H.; Blanc, A.; Weibel, J.-M.; Pale, P. Versatile and Expeditious Synthesis of Aurones via Au^{I}-Catalyzed Cyclization. *J. Org. Chem.* **2008**, *73*, 1620−1623. (e) Renault, J.; Qian, Z.; Uriac, P.; Gouault, N. Electrophilic carbon transfer in gold catalysis: synthesis of substituted chromones. *Tetrahedron Lett.* **2011**, *52*, 2476−2479. (f) Ghosh, J.; Biswas, P.; Sarkar, T.; Bandyopadhyay, C. Iodine-induced efficient construction of a chromone-linked furo-[3,2-c]chromene scaffold by a one-pot 3-component cascade reaction. *Tetrahedron Lett.* **2015**, *56*, 7193−7196. (g) Akram, M. O.; Bera, S.; Patil, N. T. A facile strategy for accessing 3-alkynylchromones through gold-catalyzed alkynylation/cyclization of *o*-hydroxyarylenaminones. *Chem. Commun.* **2016**, *52*, 12306−12309. (h) Baruah, S.; Kaishap, P. P.; Gogoi, S. Ru(II)-Catalyzed C−H activation and annulation of salicylaldehydes with monosubstituted and disubstituted alkynes. *Chem. Commun.* **2016**, *52*, 13004−13007.

(6) (a) Yoshida, M.; Fujino, Y.; Saito, K.; Doi, T. Regioselective synthesis of flavone derivatives via DMAP-catalyzed cyclization of o-alkynoylphenols. *Tetrahedron* **2011**, *67*, 9993−9997. (b) Yoshida, M.; Saito, K.; Fujino, Y.; Doi, T. A concise synthesis of 3- aroylflavones via Lewis base 9-azajulolidine-catalyzed tandem acyl transfer−cyclization. *Chem. Commun.* **2012**, *48*, 11796−11798. (c) Dubrovskiy, A. V.; Larock, R. C. Intermolecular C-O addition of carboxylic acids to arynes: synthesis of *o*-hydroxyaryl ketones, xanthones, 4-chroma-

https://dx.doi.org/10.1021/acs.organomet.0c00048
Organometallics XXXX, XXX, XXX−XXX

nones, and flavones. *Tetrahedron* **2013**, *69*, 2789−2798. (d) Castillo-Contreras, E. B.; Dake, G. R. DMAP Promoted Tandem Addition Reactions Forming Substituted Tetrahydroxanthones. *Org. Lett.* **2014**, *16*, 1642−1645. (e) Yoshida, M.; Saito, K.; Fujino, Y.; Doi, T. A concise total synthesis of biologically active frutinones via tributylphosphine-catalyzed tandem acyl transfer-cyclization. *Tetrahedron* **2014**, *70*, 3452−3458. (f) Saito, K.; Yoshida, M.; Doi, T. An Efficient Synthesis of Aurone Derivatives by the Tributylphosphine-catalyzed Regioselective Cyclization of *o*-Alkynoylphenols. *Chem. Lett.* **2015**, *44*, 141−143. (g) Zhai, D.; Chen, L.-Z.; Jia, M.-Q.; Ma, S.-M. One Pot Synthesis of γ-Benzopyranones via Iron-Catalyzed Aerobic Oxidation and Subsequent 4-Dimethylaminopyridine Catalyzed 6-*endo* Cyclization. *Adv. Synth. Catal.* **2018**, *360*, 153−160.

(7) (a) Torii, S.; Okumoto, H.; Xu, L. H.; Sadakane, M.; Shostakovsky, M. V.; Ponomaryov, A. B.; Kalinin, V. N. Syntheses of Chromones and Quinolones via Pd-Catalyzed Carbonylation of *o*-Iodophenols and Anilines in the Presence of Acetylenes. *Tetrahedron* **1993**, *49*, 6773−6784. (b) Bhat, A. S.; Whetstone, J. L.; Brueggemeier, R. W. Novel Synthetic Routes Suitable for Constructing Benzopyrone Combinatorial Libraries. *Tetrahedron Lett.* **1999**, *40*, 2469−2472. (c) Liang, B.; Huang, M.; You, Z.; Xiong, Z.; Lu, K.; Fathi, R.; Chen, J.; Yang, Z. Pd-Catalyzed Copper-Free Carbonylative Sonogashira Reaction of Aryl Iodides with Alkynes for the Synthesis of Alkynyl Ketones and Flavones by Using Water as a Solvent. *J. Org. Chem.* **2005**, *70*, 6097−6100. (d) Awuah, E.; Capretta, A. Access to Flavones via a Microwave-Assisted, One-Pot Sonogashira−Carbonylation−Annulation Reaction. *Org. Lett.* **2009**, *11*, 3210−3213. (e) Chai, G.; Qiu, Y.; Fu, C.; Ma, S. Efficient Assembly of Chromone Skeleton from 2,3-Allenoic Acids and Benzynes. *Org. Lett.* **2011**, *13*, 5196−5199. (f) Cheng, G.; Qi, Y.-B.; Zhou, X.-Q.; Sheng, R.; Hu, Y.-Z.; Hu, Y.-H. One-pot Synthesis of 6-Azachromone Derivatives Through Cascade Carbonylation Sonogashira-Cyclization. *Sci. Rep.* **2017**, *7*, 4398.

(8) (a) Lin, Q.; Leong, W. K. Reaction of Pyrones with Triosmium Clusters. *Organometallics* **2003**, *22*, 3639−3648. (b) Booysen, I. N.; Maikoo, S.; Akerman, M. P.; Xulu, B. Novel ruthenium(II) and (III) compounds with multidentate Schiff base chelates bearing biologically significant moieties. *Polyhedron* **2014**, *79*, 250−257. (c) Klier, L.; Ziegler, D. S.; Rahimoff, R.; Mosrin, M.; Knochel, P. Practical Large-Scale Regioselective Zincation of Chromone Using TMPZnCl·LiCl Triggered by the Presence or Absence of $MgCl_2$. *Org. Process Res. Dev.* **2017**, *21*, 660−663. (d) Ali, R.; Guan, Y.; Leveille, A. M.; Vaughn, E.; Parelkar, S.; Thompson, P. R.; Mattson, A. E. Synthesis and Anticancer Activity of Structure Simplified Naturally Inspired Dimeric Chromenone Derivatives. *Eur. J. Org. Chem.* **2019**, *2019*, 6917−6929. (e) Kalaiarasi, G.; Rex Jeya Rajkumar, S.; Dharani, S.; Rath, N. P.; Prabhakaran, R. *In vitro* cytotoxicity of new water soluble copper(II) metallates containing 7-hydroxy-4-oxo-4*H*-chromene thiosemicarbazones. *Polyhedron* **2019**, *173*, 114120. (f) Ismail, M. B.; Booysen, I. N.; Akerman, M. P. DNA interaction studies of rhenium compounds with Schiff base chelates encompassing biologically relevant moieties. *Nucleosides, Nucleotides Nucleic Acids* **2019**, *38*, 950−971.

(9) Representative reviews in recent years: (a) Zhang, D.; Zi, G. N−heterocyclic carbene (NHC) complexes of group 4 transition metals. *Chem. Soc. Rev.* **2015**, *44*, 1898−1921. (b) Lazreg, F.; Nahra, F.; Cazin, C. S. J. Copper−NHC complexes in catalysis. *Coord. Chem. Rev.* **2015**, *293−294*, 48−79. (c) Wang, Z.; Jiang, L.; Mohamed, D. K. B.; Zhao, J.; Hor, T. S. A. N−heterocyclic carbene complexes of Group 6 metals. *Coord. Chem. Rev.* **2015**, *293−294*, 292−326. (d) Kaufhold, S.; Petermann, L.; Staehle, R.; Rau, S. Transition metal complexes with N−heterocyclic carbene ligands: From organometallic hydrogenation reactions toward water splitting. *Coord. Chem. Rev.* **2015**, *304−305*, 73−87. (e) Patil, S. A.; Patil, S. A.; Patil, R.; Keri, R. S.; Budagumpi, S.; Balakrishna, G. R.; Tacke, M. *N*-heterocyclic carbene metal complexes as bio-organometallic antimicrobial and anticancer drugs. *Future Med. Chem.* **2015**, *7*, 1305−1333. (f) Ezugwu, C. I.; Kabir, N. A.; Yusubov, M.; Verpoort, F. Metal−organic frameworks containing N−heterocyclic carbenes and their precursors. *Coord. Chem. Rev.* **2016**, *307*, 188−210. (g) Nasr, A.; Winkler, A.; Tamm, M. Anionic N−heterocyclic carbenes: Synthesis, coordination chemistry and applications in homogeneous catalysis. *Coord. Chem. Rev.* **2016**, *316*, 68−124. (h) Liu, W.; Gust, R. Update on metal N−heterocyclic carbene complexes as potential anti-tumor metallodrugs. *Coord. Chem. Rev.* **2016**, *329*, 191−213. (i) Zhong, R.; Lindhorst, A. C.; Groche, F. J.; Kühn, F. E. Immobilization of N−Heterocyclic Carbene Compounds: A Synthetic Perspective. *Chem. Rev.* **2017**, *117*, 1970−2058. (j) Hameury, S.; de Frémont, P.; Braunstein, P. Metal complexes with oxygen-functionalized NHC ligands: synthesis and applications. *Chem. Soc. Rev.* **2017**, *46*, 632−733. (k) Zhao, W.; Ferro, V.; Baker, M. V. Carbohydrate−N−heterocyclic carbene metal complexes: Synthesis, catalysis and biological studies. *Coord. Chem. Rev.* **2017**, *339*, 1−16. (l) Charra, V.; de Frémont, P.; Braunstein, P. Multidentate N−heterocyclic carbene complexes of the 3d metals: Synthesis, structure, reactivity and catalysis. *Coord. Chem. Rev.* **2017**, *341*, 53−176. (m) Vivancos, Á.; Segarra, C.; Albrecht, M. Mesoionic and Related Less Heteroatom-Stabilized N−Heterocyclic Carbene Complexes: Synthesis, Catalysis, and Other Applications. *Chem. Rev.* **2018**, *118*, 9493−9586. (n) Kuwata, S.; Hahn, F. E. Complexes Bearing Protic N−Heterocyclic Carbene Ligands. *Chem. Rev.* **2018**, *118*, 9642−9677. (o) Wang, W.; Cui, L.; Sun, P.; Shi, L.; Yue, C.; Li, F. Reusable N−Heterocyclic Carbene Complex Catalysts and Beyond: A Perspective on Recycling Strategies. *Chem. Rev.* **2018**, *118*, 9843−9929. (p) Cheng, J.; Wang, L.; Wang, P.; Deng, L. High-Oxidation-State 3d Metal (Ti−Cu) Complexes with N−Heterocyclic Carbene Ligation. *Chem. Rev.* **2018**, *118*, 9930−9987. (q) Roland, S.; Suarez, J. M.; Sollogoub, M. Confinement of Metal−N−Heterocyclic Carbene Complexes to Control Reactivity in Catalytic Reactions. *Chem. - Eur. J.* **2018**, *24*, 12464−12473. (r) Elie, M.; Renaud, J.-L.; Gaillard, S. N−Heterocyclic carbene transition metal complexes in light emitting devices. *Polyhedron* **2018**, *140*, 158−168. (s) Hussaini, S. Y.; Haque, R. A.; Razali, M. R. Recent progress in silver(I)−, gold(I)/(III)− and palladium(II)−N−heterocyclic carbene complexes: A review towards biological perspectives. *J. Organomet. Chem.* **2019**, *882*, 96−111.

(10) (a) Chung, L.-H.; Wong, C.-Y. Isolation of Ruthenium−Indolizine Complexes: Insight into the Metal-Induced Cycloisomerization of Propargylic Pyridines. *Organometallics* **2013**, *32*, 3583−3586. (b) Chung, L.-H.; Yeung, C.-F.; Ma, D.-L.; Leung, C.-H.; Wong, C.-Y. Metal−Indolizine Zwitterion Complexes as a New Class of Organometallic Material: a Spectroscopic and Theoretical Investigation. *Organometallics* **2014**, *33*, 3443−3452. (c) Tsui, W.-K.; Chung, L.-H.; Tsang, W.-H.; Yeung, C.-F.; Chiu, C.-H.; Lo, H.-S.; Wong, C.-Y. Synthesis, Spectroscopic and Theoretical Studies of Ruthenafuran and Osmafuran Prepared by Activation of Ynone in Alcohol. *Organometallics* **2015**, *34*, 1005−1012. (d) Yeung, C.-F.; Chung, L.-H.; Lo, H.-S.; Chiu, C.-H.; Cai, J.; Wong, C.-Y. Isolation of Ruthenium−Indoline and − Indole Zwitterion Complexes: Insight into the Metal-Induced Cyclization of Aniline-Tethered Alkynes and Strategy to Lower the Activation Barrier of Metal−Vinylidene Formation. *Organometallics* **2015**, *34*, 1963−1968. (e) Ng, S.-W.; Chung, L.-H.; Yeung, C.-F.; Lo, H.-S.; Shek, H.-L.; Kang, T.-S.; Leung, C.-H.; Ma, D.-L.; Wong, C.-Y. Metalated Chromene and Chromone Complexes: pH Switchable Metal−Carbon Bonding Interaction, Photo-triggerable Chromone Delivery Application, and Antioxidative Activity. *Chem. - Eur. J.* **2018**, *24*, 1779−1783. (f) Chung, L.-H.; Ng, S.-W.; Yeung, C.-F.; Shek, H.-L.; Tse, S.-Y.; Lo, H.-S.; Chan, S.-C.; Tse, M.-K.; Yiu, S.-M.; Wong, C.-Y. Ruthenium−indolizinone complexes as a new class of metalated heterocyclic compounds: insight into unconventional alkyne activation pathways, revelation of unexpected electronic properties and exploration of medicinal application. *Dalton Trans.* **2018**, *47*, 12838−12842. (g) Chung, L.-H.; Wong, C.-Y. Ruthenium-Induced Alkyne Cycloisomerization: Construction of Metalated Heterocycles, Revelation of Unconventional Reaction Pathways, and Exploration of Functional Applications. *Chem. - Eur. J.* **2019**, *25*, 2889−2897. (h) Yeung, C.-F.; Chung, L.-H.; Ng, S.-W.; Shek, H.-L.; Tse, S.-Y.; Chan, S.-C.; Tse, M.-K.; Yiu, S.-M.; Wong, C.-Y. Phosphonium-Ring-Fused Bicyclic Metallafuran Complexes of Ruthenium and Osmium.

Chem. - Eur. J. **2019**, *25*, 9159−9163. (i) Chung, L.-H.; Yeung, C.-F.; Shek, H.-L.; Wong, C.-Y. Isolation of a C3-metalated indolizine complex and a phosphonium ring-fused bicyclic metallafuran from the osmium-induced transformation of pyridinetethered alkynes. *Faraday Discuss.* **2019**, *220*, 196−207. (j) Aoki, Y.; Bauer, M.; Braun, T.; Cadge, J. A.; Clarke, G. E.; Durand, D. J.; Eisenstein, O.; Gallarati, S.; Greaves, M.; Harvey, J.; Haynes, A.; Hintermair, U.; Hulme, A. N.; Ishii, Y.; Jakoobi, M.; Jensen, V. R.; Kennepohl, P.; Kuwata, S.; Lei, A.; Lloyd-Jones, G.; Love, J.; Lynam, J.; Macgregor, S.; Morris, R. H.; Nelson, D.; Odom, A.; Perutz, R.; Reiher, M.; Renny, J.; Roithova, J.; Schafer, L.; Scott, S.; Seavill, P. W.; Slattery, J.; Takao, T.; Walton, J.; Wilden, J. D.; Wong, C.-Y.; Young, T. Mechanistic insight into organic and industrial transformations: general discussion. *Faraday Discuss.* **2019**, *220*, 282−316.

(11) Keller, A.; Jasionka, B.; Głowiak, T.; Ershov, A.; Matusiak, R. Cyclic oxycarbene and vinylidene complexes of ruthenium with (P−P) and (N−N) type ligands. *Inorg. Chim. Acta* **2003**, *344*, 49−60.

(12) (a) Hodge, A. J.; Ingham, S. L.; Kakkar, A. K.; Khan, M. S.; Lewis, J.; Long, N. J.; Parker, D. G.; Raithby, P. R. Donor-acceptor-based vinylidene and σ-acetylide complexes of ruthenium and osmium. *J. Organomet. Chem.* **1995**, *488*, 205−210. (b) Colbert, M. C. B.; Lewis, J.; Long, N. J.; Raithby, P. R.; Younus, M.; White, A. J. P.; Williams, D. J.; Payne, N. N.; Yellowlees, L.; Beljonne, D.; Chawdhury, N.; Friend, R. H. Synthesis and Characterization of Dinuclear Metal σ-Acetylides and Mononuclear Metal σ-Allenylidenes. *Organometallics* **1998**, *17*, 3034−3043. (c) Cifuentes, M. P.; Humphrey, M. G.; Koutsantonis, G. A.; Lengkeek, N. A.; Petrie, S.; Sanford, V.; Schauer, P. A.; Skelton, B. W.; Stranger, R.; White, A. H. Coordinating Tectons: Bipyridyl Terminated Allenylidene Complexes. *Organometallics* **2008**, *27*, 1716−1726.

(13) Chung, L.-H.; Yeung, C.-F.; Wong, C.-Y. Ruthenium-Induced Cyclization of Heteroatom-Functionalized Alkynes: Progress, Challenges and Perspectives. *Chem. - Eur. J.* **2020**, DOI: 10.1002/chem.201905506.

(14) Sullivan, B. P.; Meyer, T. J. Comparisons of the Physical and Chemical Properties of Isomeric Pairs. 2. Photochemical, Thermal, and Electrochemical Cis-Trans Isomerizations of M-$(Ph_2PCH_2PPh_2)_2Cl_2$ (M = Ru^{II}, Os^{II}). *Inorg. Chem.* **1982**, *21*, 1037−1040.

(15) Schraml, J.; Čapka, M.; Blechta, V. ^{31}P and ^{13}C NMR spectra of cyclohexylphenylphosphines, tricyclohexylphosphine and triphenylphosphine. *Magn. Reson. Chem.* **1992**, *30*, 544−547.

(16) (a) Mann, A.; Muller, C.; Tyrrell, E. A diastereoselective cobalt-mediated synthesis of benzopyrans using a novel variation of an intramolecular Nicholas reaction in the key cyclisation step: optimization and biological evaluation. *J. Chem. Soc., Perkin Trans. 1* **1998**, 1427−1438. (b) Zheng, M.; Wu, F.; Chen, K.; Zhu, S. Styrene as 4π-Component in Zn(II)-Catalyzed Intermolecular Diels− Alder/Ene Tandem Reaction. *Org. Lett.* **2016**, *18*, 3554−3557.

(17) Mosmann, T. Rapid Colorimetric Assay for Cellular Growth and Survival: Application to Proliferation and Cytotoxicity Assays. *J. Immunol. Methods* **1983**, *65*, 55−63.

(18) (a) Brand-Williams, W.; Cuvelier, M. E.; Berset, C. Use of a Free Radical Method to Evaluate Antioxidant Activity. *Lebensm. Wiss. Technol.* **1995**, *28*, 25−30. (b) Nenadis, N.; Wang, L.-F.; Tsimidou, M.; Zhang, H.-Y. Estimation of Scavenging Activity of Phenolic Compounds Using the $ABTS^{\bullet+}$ Assay. *J. Agric. Food Chem.* **2004**, *52*, 4669−4674.

https://dx.doi.org/10.1021/acs.organomet.0c00048
Organometallics XXXX, XXX, XXX−XXX